HHS Public Access

Author manuscript

*Cytotherapy*. Author manuscript; available in PMC 2022 March 14.

Published in final edited form as:

*Cytotherapy*. 2020 November ; 22(11): 617–628. doi:10.1016/j.jcyt.2020.07.003.

# Identification and Characterization of a large Source of Primary mesenchymal stem cells tightly adhered to bone Surfaces of human vertebral body marrow cavities

**Brian H. Johnstone**[1,2,*], **Hannah M. Miller**[1,2], **Madelyn R. Beck**[4], **Dongsheng Gu**[1,3], **Sreedhar Thirumala**[4], **Michael LaFontaine**[2], **Gerald Brandacher**[5], **Erik J. Woods**[1,2,4,*]

[1]Ossium Health, Inc, Indianapolis, Indiana, USA

[2]Department of Biomedical Sciences, College of Osteopathic Medicine, Marian University, Indianapolis, Indiana, USA

[3]Wells Center for Pediatric Research, Indiana University School of Medicine, Indianapolis, Indiana, USA

[4]Department of Medical and Molecular Genetics, Indiana University School of Medicine, Indianapolis, Indiana, USA

[5]Department of Plastic and Reconstructive Surgery, Johns Hopkins University School of Medicine, Baltimore, Maryland, USA

## Abstract

**Background:** Therapeutic allogeneic mesenchymal stromal cells (MSCs) are currently in clinical trials to evaluate their effectiveness in treating many different disease indications. Eventual commercialization for broad distribution will require further improvements in manufacturing processes to economically manufacture MSCs at scales sufficient to satisfy projected demands. A key contributor to the present high cost of goods sold for MSC manufacturing is the need to create master cell banks from multiple donors, which leads to variability in large-scale manufacturing runs. Therefore, the availability of large single donor depots of primary MSCs would greatly benefit the cell therapy market by reducing costs associated with manufacturing.

**Methods:** We have discovered that an abundant population of cells possessing all the hallmarks of MSCs is tightly associated with the vertebral body (VB) bone matrix and only liberated by proteolytic digestion. Here we demonstrate that these vertebral bone-adherent (vBA) MSCs possess all the International Society of Cell and Gene Therapy-defined characteristics (e.g.,



*Correspondence: Brian H. Johnstone, PhD and Erik J. Woods, PhD, HCLD(ABB), Ossium Health, Inc, 5754 W 74th St, Indianapolis, Indiana 46278, USA. brian.johnstone@ossiumhealth.com (B.H. Johnstone), erik@ossiumhealth.com (E.J. Woods).

Author Contributions

Conception and design of the study: BHJ and EJW Acquisition of data: HMM, MB, DG, ST, Analysis and interpretation of data: BHJ, HMM, DG, ST, ML, GB, EJW Drafting or revising the manuscript: BHJ, EJW, ML, GB. All authors have approved the final article.

Declaration of Competing Interest

The authors have no commercial, proprietary or financial interest in the products or companies described in this article.

Supplementary materials

Supplementary material associated with this article can be found in the online version at doi:10.1016/j.jcyt.2020.07.003.

plastic adherence, surface marker expression and trilineage differentiation) of MSCs, and we have therefore termed them vBA-MSCs to distinguish this population from loosely associated MSCs recovered through aspiration or rinsing of the bone marrow compartment.

**Results:** Pilot banking and expansion were performed with vBA-MSCs obtained from 3 deceased donors, and it was demonstrated that bank sizes averaging $2.9 \times 10^8 \pm 1.35 \times 10^8$ vBA-MSCs at passage 1 were obtainable from only 5 g of digested VB bone fragments. Each bank of cells demonstrated robust proliferation through a total of 9 passages, without significant reduction in population doubling times. The theoretical total cell yield from the entire amount of bone fragments (approximately 300 g) from each donor with limited expansion through 4 passages is 100 trillion ($1 \times 10^{14}$) vBA-MSCs, equating to over $10^5$ doses at $10 \times 10^6$ cells/kg for an average 70-kg recipient.

**Discussion:** Thus, we have established a novel and plentiful source of MSCs that will benefit the cell therapy market by overcoming manufacturing and regulatory inefficiencies due to donor-to-donor variability.

### Keywords

bone marrow; cellular therapy; large-scale manufacturing; human MSCs; regenerative medicine; vertebral bodies

## Introduction

The potent activity as well as high expandability of mesenchymal stromal cells (MSCs) has garnered considerable attention from commercial entities interested in developing “off-the-shelf” allogeneic MSC therapeutics derived from a limited number of donors. Development of a cellular therapy based on allogeneic universal donors allows for controlled manufacture, with attention given to a thorough assessment of the quality (e.g., identity, potency, purity and safety) of each manufactured lot, at significant cost savings compared with manufacturing individual lots of autologous cells from individual donors, such as currently occurs with chimeric antigen receptor T-cell therapies.

The challenges inherent to manufacturing cellular therapies scale with the size of a manufacturing run. Effective doses of MSCs for some indications are as high as $1 \times 10^9$ cells per dose, which would require manufacturing 10 trillion ($10 \times 10^{12}$) cells per year to affordably meet potential demand [1–4]. Even at this level of production, with presumed economies of scale, the cost of goods sold (COGS) per dose of MSCs could exceed $100,000 [3].Asignificant driver of manufacturing costs, which is amplified proportionately with lot size, is the need to replenish master cell banks (MCBs) through isolation of MSCs from new donors because of the limited volume of tissues and fluids that can be safely obtained from healthy volunteers and the limited expansion potential of MSCs isolated from each donor [5,6]. MSCs are rare in all tissues, comprising, for instance, ~0.001–0.01% of total nucleated cells in bone marrow (BM) aspirates [7]. Given that BM aspirates from healthy volunteers are limited for the safety of the donor to 100 mL (50 mL bilaterally from the iliac crests), the total yield of fresh, non-passaged MSCs is approximately $2 \times 10^4$ per donor. Expansion to a trillion cells would require seed stocks of $1 \times 10^7$MSCs to limit cell

proliferation to 9 population doublings [8]. This number is in addition to the cells reserved for quality control measurements of the expanded MCBs and working cell bank (WCB). Thus, the number of MSCs obtainable from each donor is more than 3 orders of magnitude less than is optimal for the initial stages of expansion.

The need to constantly replenish cell banks by obtaining fresh cells from new donors introduces inconsistencies into the manufacturing process due to the observed variability between MSCs derived from different donors otherwise matched for attributes such as age and health status [6,9,10]. Donor-to-donor variability and the resulting economic impact on manufacturing costs are substantial. In one study that examined large-scale manufacturing of multiple lots of MSCs derived from different donors, it was found that cumulative population doublings between 5 different BM donors varied by 1.8-fold during 30 days in culture [9]. The result was a > 13-day variation in process time to manufacture a batch of 350 million MSCs. Besides the logistical burden to coordinate batch runs, there was a commensurate increased cost of growth medium, which is also a key cost driver for cell-based therapy manufacturing [1,3,8]. Furthermore, the authors found that there was a > 18% difference in colony-forming potential and a > 50% difference in IL-6 expression, adding an additional complication to quality control verification of potency for each batch derived from individual donors. Similarly, during clinical manufacture of 68 batches of MSCs from BM recovered from 59 human volunteer donors, a single center observed population doubling times that varied by over 2-fold (46.8–141 h, averaging 71.7 h), yielding final batch numbers of MSCs ranging from $1.9 \times 10^7$ to $5.43 \times 10^9$ (average $5.46 \times 10^8$) [10].

Besides imposing a direct economic burden of increasing COGS per manufacturing run, there is also a regulatory burden, with associated costs resulting from the need to refresh cell banks. The MCB serves as the reserve of starter cultures for all manufacturing runs using cells from a particular donor. The regulatory requirements for quality and safety assessments of the MCBs are costly and time-consuming [11]. Of the 3 overarching parameters (i.e., safety, potency and identity) required to assess suitability of a manufactured cell therapy product, potency, as it relates to individual donor characteristics, is most problematic because of the changing profile that occurs with expansion, as described earlier. This is particularly the case as MSC populations near the limits of expansion and enter into senescence, which severely limits their potency [12]. For these reasons, population doubling limit is an important factor for regulatory authorities, albeit one that is not commonly addressed in filings with the Food and Drug Administration [13].

Reducing the economic and regulatory burden of generating multiple MCB lots annually to fulfill the need for large-scale manufacturing requires identifying large depots of unmanipulated MSCs. Potential solutions could come from abundant tissues harboring MSCs that are normally discarded following routine medical procedures or are obtainable postmortem. Adipose-derived stem/stromal cells are obtained from elective procedures that commonly yield liters of tissue and have recently been extensively investigated; however, this is primarily for autologous uses [14,15]. Isolation directly from medullary cavity-containing bones obtained through medical procedures or cadavers yields higher percentages of MSCs (~0.04%) than are present in aspirates, most likely reflecting lack of peripheral blood contamination [16]. Total nucleated cell counts of $\sim 5 \times 10^9$ have been obtained

from BM of vertebral bodies (VBs) recovered from deceased organ donors, with each VB containing ~$2 \times 10^6$ MSCs, or ~$2 \times 10^7$ total MSCs per typical spinal 9 VB segment recovered [17]. In addition, the ilia, sternum, ribs and heads of long bones are sources of BM from which MSCs can be recovered [18–20]. Thus, the VB compartment of BM from a typical deceased donor yields > 3 orders of magnitude more MSCs than can be obtained from a healthy human donor.

In addition to cells obtained by eluting or aspirating BM, another population of MSCs is tightly associated with medullary cavity bone structures [21–23]. First identified in rodent long bones, bone-adherent MSCs (BA-MSCs) have subsequently been isolated from human bone fragments obtained from long bone condyles and vertebrae [24]. We have discovered another source of MSCs called vertebral BA-MSCs (vBA-MSCs), which remain attached to fragments of VB bone after extensive washing to remove BM cells and can only be liberated by digestion with proteases. The frequency and functionality of vBA-MSCs are equivalent to that seen in eluted VB BM-MSCs. Here we present these data and establish a new source of MSCs that could be used in large-scale manufacturing processes to produce batches totaling over a quadrillion cells from an individual donor, thus satisfying the most optimistic levels of demand for decades and overcoming a current impediment to commercial scale production [2,8].

## Methods

### Sources of tissues and Cells

Vertebrae were recovered from organ donors who consented in life with consent re-affirmed by next of kin for research use. All donors were recovered by licensed United States Organ Procurement Organizations. As deceased donors, based on FDA 45 CFR 46.102 and 21 CFR 56.102, the activities described in this project do not constitute human subjects research. Each recovered vertebra was deidentified and assigned a unique identifier. The inclusion criteria for donor selection were brain death, age within the range of 12 and 55 years, non-septicemic and disease- and pathogen-free. Live donor aspirated BM from 3 healthy volunteers was purchased from Lonza (Walkers-ville, MD, USA). Expanded live donor MSCs, cryopreserved at passage 2, were purchased from Lonza. Relevant donor characteristics are presented in Table 1.

### Deceased donor tissue procurement and transport

Previously developed clinical recovery methods [16,25], combined with subsequent experience in the ongoing vascularized composite allograft transplant immunomodulation clinical trial (ClinicalTrials.gov Identifier: NCT01459107) at Johns Hopkins University, formed the basis for the procurement and transport protocols. A streamlined organ procurement organization (OPO) recovery procedure, combined with dedicated kits and centralized training on recovery and shipment procedures, was employed. Recovered bones were shipped to Ossium Health (Indianapolis, IN, USA). Vertebral sections were procured by 5 different OPO partners: MidWest Transplant Network (Westwood, KS, USA), Mid America Transplant (St Louis, MO, USA), Donor Network West (San Ramon, CA, USA), Washington Regional Transplant Community (Falls Church, VA, USA), and LifeShare of the

Carolinas (Charlotte, NC). Bones were recovered by OPO personnel using an osteotome and mallet. Recovered bones were wrapped in lap sponges and towels soaked in saline to ensure moisture retention during shipment. Wrapped specimens were shipped overnight on wet ice to Ossium's processing facility.

### Manual debridement

Upon receipt, in a biological safety cabinet, soft tissue was manually debrided using scalpels and gouges. Once visible, the pedicles were removed using a Stryker System 6 saw (Stryker, Kalamazoo, MI, USA), leaving only the connected vertebral bodies. Vertebral bodies were separated, and intervertebral disk and soft tissue were removed with a scalpel. Care was taken to ensure that the cortical bone was not breached to preserve and protect the hypoxic cancellous bone marrow throughout the entire debriding process.

Using custom-made surgical-grade stainless steel anvil shears, VBs were cut into approximately 5 $cm^3$pieces, small enough to be fragmented with a bone grinder. The pieces were immediately submerged into 500 mL processing medium comprised of Plasma-Lyte A pH 7.4 (Baxter Healthcare, Deerfield, IL, USA) containing 2.5% human serum albumin (Octapharma USA Inc, Hoboken, NJ, USA), 3 U/mL Benzonase (EMD Millipore, Burlington, MA, USA) and 10 U/mL heparin (McKesson, Irving, TX, USA).

### Grinding and elution

A bone grinder (Biorep Technologies, Inc, Miami, FL, USA) was assembled in a biological safety cabinet. A 2-L stainless steel beaker containing approximately 250 mL of fresh processing medium was placed under the grinding head to catch bone chips and media flow-through. A stainless steel plunger was used to aid in pushing pieces through the grinder. Rinsing through the grinder with processing medium prevented bone pieces from drying out and sticking to the chamber. Once all bone pieces were ground, the chamber was thoroughly rinsed with fresh processing medium. The final volume in the stainless steel beaker was 1 L.

Filtering was performed using bone marrow collection kits with flexible pre-filter and inline filters (Fresenius Kabi, Lake Zurich, IL, USA). All bone grindings and media were carefully transferred to the bone marrow collection kit. The grindings were gently massaged to allow for optimal cell release. The media were then filtered using two 500-μm and two 200-μm filters. The bone grindings were rinsed using two 500-mL washings with rinse media. Rinse medium was Plasma-Lyte (Baxter Healthcare) with 2.5% human serum albumin. All bone marrow was then collected in a collection bag. The bone fragments remaining in the filtration kit were stored at 4°C overnight before processing to recover vBA-MSCs.

### Digestion protocol for vBA-MSC isolation

Bone fragments (either 1 or 5 g) were transferred to sterile 50-mL conical centrifuge tubes. A solution of collagenase 2 mg/mL (DE10, Vitacyte, Indianapolis, IN, USA) was added to the bone fragments at a ratio of 5:1 (volume to weight). The tubes were transferred to a shaking incubator and incubated for 1.5 h at 37°C while shaking at 125 rpm. Protease activity was neutralized by adding 2% Stemulate (Cook Regentec, Indianapolis, IN, USA),

and suspensions were filtered through a 70-μm capfilter into 50-mL conical screw cap tubes. The filter-retained bone fragments were washed with 25 mL Dulbecco's Phosphate-Buffered Saline (DPBS) solution containing heparin 10 U/mL and Benzonase 100 U/mL (EMD Millipore), which was combined with the original filtrate. Tubes were centrifuged at 350 × g for 5 min, the supernatant was aspirated and the pellets were resuspended in 25 mL DPBS. The suspension was centrifuged again at 350 × g for 5 min, the supernatant was aspirated and the pellets were resuspended in 10 mL DPBS for analysis.

### Isolation of MSCs from iliac and VB BM

A 1-mL aliquot of concentrated eluted BM was removed and pipetted into a 50-mL conical vial along with 49 mL DPBS. The vial was centrifuged at 300 × g for 10 min, the supernatant was aspirated and the pellets were resuspended in 10 mL RoosterNourish medium (RoosterBio, Frederick, MD, USA). Cells were counted and cultured as described in the following sections.

### Cell counting

A Cellometer Vision (Nexcelom, Lawrence, MA, USA) was used to determine total viable cell counts. Then 20 μL ViaStain AOPI reagent (Nexcelom) was added to an Eppendorf tube containing 20 μL of cells. Once mixed, 20 μL of the solution was added to a Cellometer slide, and total cells, live cells and viability were calculated.

### Cell culture

Fresh cells were plated in CellBIND T-225 flasks (Corning, Tewksbury, MA, USA) at a density of 25 000 viable cells/cm$^2$ in RoosterNourish medium (RoosterBio). Nonadherent cells were removed after the first media change on day 1. Media were then changed every 3–4 days until colonies were ~80–90% confluent (12–14 days). Cells were released with TrypLE (Thermo Fisher Scientific, Waltham, MA, USA). Passaged cells were plated at a density of 3000 cells/cm$^2$ but otherwise followed the same protocol as freshly plated cells.

Generation of MCBs from 3 deceased donors (DD5, DD6 and DD7) was performed in CellBIND HYPERFlasks. Fresh, primary digests were initially plated at 25 000 viable cells/cm$^2$ as described earlier. Cells were released with TrypLE and expanded one more passage to form the MCBs. The bulk of passage 1 cells were resuspended in cryopreservation medium (CryoStor CS10; BioLife Solutions, Inc, Bothell, WA, USA) and stored in the vapor phase of liquid nitrogen.

Cells were passaged up to 9 times in a medium composed of Dulbecco's Modified Eagle's Medium (Cat#10567014; Thermo Fisher) and pathogen-reduced human platelet lysate (nLivenPR; Cook Regentec), with and without the addition of ascorbic acid 248 mM (Cat# A2218; Sigma-Aldrich), recombinant basic fibroblast growth factor 10 ng/mL (Cat#233-GMP-025; R&D Systems, Inc, Minneapolis, MN, USA) and recombinant epidermal growth factor 10 ng/mL (Cat#236-GMP-200; R&D Systems, Inc). Cells at 70–80% confluency were harvested, and total cell counts were obtained. A portion of the cells was replated to at 3000 cells/cm$^2$in triplicate wells of a 6-well plate, with media changes every 3–4 days.

### Phenotypic analysis of MSCs via flow cytometry

At passages 2, 3 and 4, 1.8 μL of CD3, CD14, CD19, CD31, CD34, CD45, HLA-DR, CD73, CD90, CD105, STRO-1 and 7-aminoactinomycin D single fluorescently conjugated antibodies and dye, respectively (see supplementary Table 1), were added to different wells of a 96-well V-bottom plate; 100 μL of MACS (Miltenyi Biotec, Auburn, CA, USA) buffer and 100 μL of cells (200 000 cells) were added to each well containing an antibody. The plate was incubated at 4°C for 30 min, shielded from light, and afterward was centrifuged for 5 min at 300 × g. Cells were washed and resuspended in 200 μL of MACS (Miltenyi Biotec) buffer. A NovoCyte 2060R flow cytometer (ACEA Biosciences, San Diego, CA, USA) was used for data collection, and data were analyzed using NovoExpress software (ACEA Biosciences).

### Trilineage differentiation of MSCs

MSCs at passages 1 and 3 were seeded in wells of a 12-well plate containing 3 mL MesenCult (Stem Cell Technologies, Vancouver, Canada), each at $8.0 \times 10^4$, $4.0 \times 10^4$ and $2.0 \times 10^4$ for chondrogenesis, adipogenesis and osteogenesis differentiation. Wells containing 4.0 £ 104 MSCs in MesenCult medium (Stem Cell Technologies) served as controls. After incubating for 2 h, MesenCult (Stem Cell Technologies) in the chondrogenesis well was replaced with StemPro chondrogenesis medium (Thermo Fisher Scientific, Waltham, MA, USA). After 1 day, MesenCult (Stem Cell Technologies) in the adipogenesis and osteogenesis wells was aspirated and replaced with StemPro (Thermo Fisher Scientific) adipogenesis medium and StemPro (Thermo Fisher Scientific) osteogenesis medium, respectively. Respective differentiation media were replenished every 3 days, as was MesenCult in the control wells. After 14, 12 and 16 days, wells containing chondrocytes, adipocytes and osteocytes were aspirated of media, washed twice with DPBS, fixed with 4% formalin for 30 min, washed once with DPBS and stained. Alcian Blue, which stains chondrocyte proteoglycans blue, in 0.1 N HCl was added to the chondrocyte wells for 30 min, the stain was aspirated, the well was washed 3 times with 0.1 N HCl and neutralized with distilled water and chondrocytes were visualized under an inverted light microscope (Nikon). Oil Red O, which stains adipocyte fat globules red, was added to the adipocyte well for 15 min, the stain was aspirated, the well was washed 3 times with distilled water and adipocytes were visualized under an inverted light microscope. Then 2% Alizarin Red, which stains osteocyte calcium deposits red, was added to the osteocyte well for 3 min, the stain was aspirated, the well was washed 3 times with distilled water and osteocytes were visualized under an inverted light microscope. All differentiated cells were qualitatively analyzed by visualization of color and morphology.

### Quantitative real-time polymerase chain reaction analysis of gene expression during differentiation

RNA was isolated from differentiated cells using TRIzol RNA isolation reagents (Invitrogen, USA), and complementary DNA was produced using a high-capacity complementary DNA reverse transcription kit (Applied Biosystems, USA). The primers (see supplementary Table 2) were obtained from Integrated DNA Technologies, Inc (USA), and were used to measure the gene expressions of the adipogenesis-related proteins lipoprotein lipase and fatty acid

binding protein 4; the osteogenesis-related proteins osteonectin, osteopontin and collagen type 1; and the chondrogenesis-related proteins aggrecan, collagen type 2 and SOX9. Real-time polymerase chain reaction assays were run on the Bio-Rad C1000 Touch (BioRad, USA) real-time polymerase chain reaction system. The data were analyzed relative to the housekeeping gene, *GAPDH*, and then the fold change of the gene in differentiated cells was calculated relative to undifferentiated cells.

### Population doubling time

Population doubling time (PDT) was determined at each passage using the formula t*log(2)/log($T_1$ /$T_0$), where t is the time (h) between initial plating and cell harvest at 90% confluency, $T_1$ is the cell count at harvest and $T_0$ is the initial count at seeding.

### Colony-forming unit fibroblast assays

For freshly digested cells, 5 mL MesenCult (Stem Cell Technologies), 20 μL amphotericin B and 100 μL gentamicin were added to 3 wells of a 6-well plate, and 2.5 × $10^5$, 5.0 μ $10^5$ and 7.5 μ $10^5$ cells were added to the first, second and third wells, respectively. Plates were placed in the incubator until colonies were 90% confluent, or up to 12 days. Media were changed every 3–4 days for 14 days. Plates were washed twice with DPBS, and 2 mL methanol was added to each dish for 5 min to fix the cells. After 5 min, the methanol was decanted, the plate was allowed to air dry and colonies were stained with a 1% Crystal Violet solution. Colonies containing > 50 cells were scored. Passaged cells were assayed similarly, except that cells were plated at densities of 32 cells/$cm^2$, 65 cells/$cm^2$ and 125 cells/$cm^2$.

### T-cell suppression assays

Suppression of T-cell activation was performed according to previously published protocols with minor modifications [26].Briefly, peripheral blood mononuclear cells (PBMCs) were isolated from whole blood (10 mL) by Ficoll (Sigma-Aldrich) separation and resuspended in DPBS. The majority of cells were labeled with carboxyfluorescein diacetate succinimidyl ester (Sigma-Aldrich) and frozen until used [27]. Passage 2 and 3 MSCs, in some cases pre-stimulated with 100 ng/mL interferon-γ (IFN-γ) (R&D Systems, Inc)for 18–24 h, were resuspended in RoosterNourish (RoosterBio) and added to a 96-well flat-bottom plate at 4 × $10^5$, 1 × $10^5$, 5 × $10^4$, 2.5 ×$10^4$, 1.5 ×$10^4$ and 5 × $10^3$ cells/well. RoosterNourish was added to each well until the volume was 200 mL/well. The plate was placed in a 37°C incubator with 10% $CO_2$ at 5% humidity for at least 2 h to allow MSCs to attach. Cryopreserved PBMCs were quickly thawed and resuspended at a concentration of 4 × $10^6$ cells/mL in Eagle's Minimal Essential Medium (Stem Cell Technologies) supplemented with 10% fetal bovine serum, 100 μg/mL penicillin-streptomycin, 2 mM L-glutamine and 100 μM β-mercaptoethanol. The medium was aspirated from the plates containing MSCs, and 100 μL of PBMCs were added to all wells containing MSCs as well as wells without MSCs. T cells were stimulated by adding 100 μL of supplemented Eagle's Minimal Essential Medium with 40 μg/mL phytohemagglutinin (PHA) (Sigma-Aldrich) to each well containing MSCs and PBMCs. Control wells containing carboxyfluorescein diacetate succinimidyl ester-labeled and unlabeled PBMCs alone were also included, half of which were stimulated with PHA and half of which were not. The plate was returned to the incubator. After 4 days, PBMCs

from each well were removed and labeled with 5 μL CD3-PE and 5 μL 7-aminoactinomycin D before performing flow cytometry

### Statistics

Prism 8 (GraphPad Software Inc, La Jolla, CA, USA) was used for statistical analysis (Student's *t*-test). $P < 0.05$ was considered significant.

## Results

A typical vertebral column (typically T8–L5) before and after removing soft tissues, separating VBs and fragmenting to sizes of approximately 1.5 $cm^3$ is shown in Figure 1. Plastic-adherent vBA-MSCs possessed a typical spindle-shaped morphology in culture (Figure 1D). Cells from donors were expanded through passage 4 (the initial plating was considered passage 0) and assayed by flow cytometry. The vBA-MSCs at passages 1–4 expressed very low levels of hematopoietic cell surface markers CD14, CD19, CD34 and CD45 and expressed low to non-existent amounts of HLA-DR (Figure 2A). The gating strategy and representative flow cytometry dot plots are shown in supplementary Figure 1. Levels of *PECAM1* (CD31)-expressing cells (typically endothelial cells and monocytes) were also low (<7%) at passage 2 (data not shown). Conversely, passaged vBA-MSCs were uniformly positive for CD73, CD90 and CD105. Thus, vBA-MSCs possess the characteristic MSC surface marker profile [28]. In addition, a variable portion (approximately 20% or less, depending on the passage number) of the population expressed the multi-potential MSC surface marker STRO-1 [29–32].

Chondrogenic, adipogenic and osteogenic potentials of passage 3 vBA-MSCs were determined for each donor. Each of the vBA-MSC isolates demonstrated the potential to differentiate into chrondrocytes, adipocytes and osteocytes, as determined by histology (Figure 2B) and quantitation of RNA transcripts associated with each differentiation pathway (Figure 2C). A portion of both freshly isolated (i.e., never plated) and passaged vBA-MSCs demonstrated high degrees of clonal proliferation, as determined by colony-forming unit fibroblast (CFU-F) potentials. The average CFU-F frequency in freshly digested VB bone fragments was 0.01% ± 0.004% (mean ± standard deviation), which is similar to the frequency of proliferative MSCs in whole BM (Figure 3) [7]. The proliferative cells were maintained with cell culture, forming colonies at a frequency of 37% ± 3.4% and 27% ± 1.2% after 1 and 2 passages, respectively.

Suppression of T-cell activation is one of the best studied therapeutic properties of MSCs, providing the rationale for testing in clinical trials of inflammatory disorders [33,34]. The vBA-MSCs from the 3 different donors dose-dependently suppressed T-cell activation with PHA (Figure 4). Maximum suppression at a 1:1 ratio of vBA-MSCs to PBMCs was 89% ± 7%. A slight but nonsignificant increase in suppression at all ratios was observed by pre-treating vBA-MSCs with IFN-γ for 18–24 h prior to performing the suppression studies. Treatment with IFN-γ has been shown to stimulate immunosuppressive functions of MSCs, with enhanced effects on senescent cells [12]. The insensitivity to priming with concentrations of IFN-γ shown previously to stimulate T-cell suppression may indicate that vBA-MSCs retain full immunomodulatory capacity during culture expansion.

The immunophenotypic profile of plastic-adherent vBA-MSCs, trilineage differentiation capacity and CFU-F potential as well as immunomodulatory properties confirm the classification of these cells as MSCs according to the published guidance of the International Society of Cell and Gene Therapy [28]. To further establish their equivalency to MSCs obtained from BM, a comparison was performed between vBA-MSCs and MSCs isolated from central BM (Figures 5, 6). Both commercially available previously expanded live donor BM-MSCs (LD Ex BM-MSCs), obtained cryopreserved at passage 2, and MSCs freshly isolated from live donor aspirated BM (LD BM-MSCs) were used. In addition, MSCs isolated from deceased donor VB BM were included in the comparison. MSCs from 3 donors for each source were expanded to passage 2 and cryopreserved. Upon subsequent thawing, cells were passaged once prior to performing the analyses. MSCs from all 4 sources demonstrated essentially identical immunophenotypic cell surface marker profiles, with very low numbers of cells that expressed CD14, CD19, CD34, CD45 and HLA-DR, and, conversely, nearly all cells expressed CD73, CD90 and CD105 (Figure 5A).

MSCs from each source grew rapidly in culture through 5 passages (the longest period examined), with no differences in PDTs at passages 4 and 5 (Figure 5C,D). The LD Ex BM-MSCs, which were obtained pre-expanded to passage 2, exhibited significantly higher PDTs at passage 3 than the other 3 MSC populations (Figure 5B). The CFU-F potential of passage 2 LD Ex BM-MSCs was also significantly lower than the other MSC populations (Figure 5E). Later passages were not compared for CFU-F potential. Finally, trilineage differentiation potentials were compared, and it was found that each MSC population formed adipocytes, chondrocytes and osteocytes *in vitro* at qualitatively the same frequencies (Figure 6).

The potential clinical translational utility of vBA-MSCs was assessed by performing a pilot-scale manufacturing run to examine feasibility of banking and expanding large numbers of cells from individual donors. Fragments of VB from 3 different donors were digested to isolate vBA-MSCs. The amount (5 g) corresponded to approximately 1/60 of the total VB bone fragment weight (300 g) obtainable from typical donors. Cells enzymatically liberated from VB fragments were plated in a Dulbecco's Modified Eagle's Medium/human platelet lysate base medium with and without the addition of growth factors and ascorbic acid (see Methods). The addition of fibroblast growth factor 2 and epidermal growth factor was required for optimal growth rate and final yields (ST, manuscript in preparation), as demonstrated previously [35]. An MCB at passage 1 from each donor, containing an average of $2.9 \times 10^8 \pm 1.35 \times 10^8$ vBA-MSCs, was prepared and the bulk cryopreserved, while the remainder was cultured over multiple passages, tracking total cell yields at each passage (Figure 7A). Passage 1 was considered to be optimal for an MCB, displaying essentially the same surface marker profile and CFU-F potential as later passages (Figures 2, 3). A single further expansion to passage 2 was enough to produce a WCB containing $5.17 \times 10^9 \pm 4.3 \times 10^9$ vBA-MSCs. Based on observed population doublings, 2 expansions of the entire WCB were sufficient to manufacture over $2 \times 10^{12}$ (2 trillion) cells. The PDT remained nearly constant between passages 2 and 9, without indications of diminishing growth rate at the upper passage number. However, there were differences in PDTs between donors (Figure 7B). Based on the observed PDTs for each donor, starting with a seed stock of 2 million vBA-MSCs, it would require 23, 36 and 29 days to manufacture 1 trillion cells from the 3

different donors. These times were calculated using 2-dimensional tissue culture flasks and would likely differ in 3-dimensional bioreactors.

## Discussion

The transformative potential of MSCs to treat a wide variety of medical disorders has been idealized for over a decade, yet despite many demonstrations of this potential in pre-clinical and early-stage clinical trials, no MSC-based therapies have achieved success in late-stage, registration (commonly phase 3 in the USA) clinical trials, although a few have received approval for limited indications in relatively small jurisdictions. The reasons for the slow progress in approvals and resulting commercialization of therapeutic MSCs despite intense development efforts by multiple entities are certainly multifactorial. In hindsight, it appears that attempts to manufacture MSCs at a large scale through adopting processes and procedures from the highly successful biopharmaceutical sector might have been a contributory factor [36,37]. There are many differences between manufacturing products derived from cells and the cells themselves. Biopharmaceuticals are produced using immortalized cell lines possessing the ability of nearly unlimited expansion, allowing the generation of large MCBs from a single seed stock. Conversely, the limited availability and expansion potential of MSCs require generating multiple MCBs from different donors each year at a disproportionately higher manufacturing cost and regulatory burden [37].

We present here a viable solution to reducing these burdens through the identification and characterization of a large depot of MSCs from deceased donor vertebral bones. Based on the analysis presented here, vBA-MSCs are phenotypically and functionally equivalent to MSCs obtained from central BM. The cells express typical MSC surface markers (CD73, CD90 and CD105) and lack expression of hematopoietic cell surface markers as well as HLA class II proteins (Figures 2, 5A). Like BM-MSCs, vBA-MSCs possess the potential to clonally expand and can be induced to undergo trilineage differentiation (Figures 2, 3, 5, 6). Passaged vBA-MSCs are fully fit to suppress T-cell activation, demonstrating no difference in activity with prior stimulation by IFN-$\gamma$ (Figure 4). The differences in PDT and CFU-F's of passage 3 (but not later passages) expanded BM-MSCs obtained from a commercial source most likely reflect a slower recovery from cryopreservation at passage 2 (Figure 5B). All MSCs were grown to passage 2 and cryopreserved in an effort to maintain comparability; however, the commercial source of expanded BM-MSCs was likely grown in a different medium and frozen in a different cryopreservation medium. Thus, the cells experienced a lag upon thaw and growth to passage 3, which was not evident in subsequent passages.

MCB sizes averaging $2.9 \pm 10^8$ passage 1 vBA-MSCs were obtainable from only approximately 1/60 (5 g) of the total digested VB bone fragments recovered from each of 3 donors (Figure 7A). The calculated total yield at passage 4 of vBA-MSCs from each donor in this study is over $1 \times 10^{14}$ (100 trillion) cells, equating to over $10^5$ doses at $10 \times 10^6$ cells/kg for an average 70-kg patient. More recent experience, following further optimization of isolation and expansion protocols, suggests that an order of magnitude greater yield at each passage is attainable (Ossium internal data). Inevitably, actual total cell yields will be lower because of inefficiencies inherent in large-scale manufacturing and requirements for

testing; nonetheless, the COGS for production of large batches of vBA-MSCs from a single donor would likely be much less than that seen with equivalent scales of manufacturing of BM-MSCs from multiple donors. The savings in direct manufacturing costs would be in addition to the reduced regulatory burden that comes with using a single donor source for all manufacturing campaigns. The next step in validating the potential cost savings with vBA-MSCs will be to perform scaled-up manufacturing runs, which are currently in progress.

We are presently exploring the question of why some populations of MSCs are easily dislodged or possibly free-floating in the BM, whereas others remain tightly adhered to the bone/connective tissue matrix and can only be liberated by enzymatic digestion. Determining differences, if they exist, is complicated by the relatively low frequency (<0.01%) of these cells, making their characterization problematic using common analytical tools, such as flow cytometry, without first expanding in culture, which induces phenotypic and functional alterations [38–46]. One previous report found that freshly isolated enzymatic digests of pelvic region trabecular bone contained 15-fold higher CFU-F's than aspirated BM [24]; however, we did not find a similar difference between freshly isolated vBA-MSCs and BM-MSCs. To better understand dissimilarities, if any, between the populations, we are pursuing single cell RNA sequencing of vBA-MSC transcriptomes [47,48]. We are also continuing to characterize the therapeutic potential of vBA-MSCs by studying the secretome and extracellular vesicles produced by these cells.

This study was restricted to characterizing vBA-MSCs from young, healthy donors between the ages of 15 and 31 years. We have also successfully isolated these cells from older donors (up to 56 years) and demonstrated expansion in culture (unpublished data). However, we intentionally focused on young donors in this article given the literature suggesting higher frequencies and proliferation rates of MSCs derived from various tissues obtained from young donors compared with their older counterparts [49–55]. Therefore, in the absence of impacts from environment and disease status, the lowest COGS to manufacture vBA-MSCs would be from young donors.

In summary, based on the data presented here, the fundamental nature of vBA-MSCs does not appear to differ from aspirated BM-MSCs; therefore, these cells could potentially be seamlessly substituted for therapeutic applications at a significant savings in manufacturing and regulatory costs. Additionally, other markets requiring large numbers of MSCs could benefit from an abundant source of primary cells. These include tissue engineering and manufacture of products derived from MSCs, such as exosomes, as well as biomedical research applications and the emerging applications of cosmeceuticals and bioengineered materials. Each of these markets is expected to grow substantially over the next decades, driving combined demand for MSCs in excess of 10 sextillion ($1 \times 10^{21}$) cells annually by 2040 [2]. Future high demand for MSCs across all these markets could be entirely met by vBA-MSCs obtained from the abundant and steady supply of deceased donor medullary cavity-containing bones from the > 10000 organ donors and > 40000 tissue donors in the USA each year alone [56].

## Supplementary Material

Refer to Web version on PubMed Central for supplementary material.

## Acknowledgments

The authors thank Jeffrey Gimble, MD, PhD, at Obatala Sciences, Inc, for providing reagents and for reviewing the manuscript. The authors also thank Nicholas Weinstein for technical assistance, and Suzanne Conrad for reviewing the mansucript.

Funding

This research was supported by grants from the National Institute of Allergy and Infectious Diseases (AI138334, AI129444) and the National Heart, Lung, and Blood Institute (HL142418) to EJW.

## References

[1]. Lipsitz YY, et al. A roadmap for cost-of-goods planning to guide economic production of cell therapy products. Cytotherapy 2017;19(12):1383–91. [PubMed: 28935190]

[2]. Olsen TR, et al. Peak MSC—Are We There Yet? Front Med (Lausanne) 2018;5:178. [PubMed: 29977893]

[3]. Pereira Chilimia TD, Moncaugeig F, Farid SS. Impact of allogeneic stem cell manufacturing decisions on cost of goods, process robustness and reimbursement. Biochemical Engineering Journal 2018;137:132–51.

[4]. Simaria AS, et al. Allogeneic cell therapy bioprocess economics and optimization: single-use cell expansion technologies. Biotechnol Bioeng 2014;111(1):69–83. [PubMed: 23893544]

[5]. Harrison RP, Medcalf N, Rafiq QA. Cell therapy-processing economics: small-scale microfactories as a stepping stone toward large-scale macrofactories. Regen Med 2018;13(2):159–73. [PubMed: 29509065]

[6]. Mizukami A, et al. Technologies for large-scale umbilical cord-derived MSC expansion: experimental performance and cost of goods analysis. Biochemical Engineering Journal 2018;135:36–48.

[7]. Pittenger MF, et al. Multilineage potential of adult human mesenchymal stem cells. Science 1999;284(5411):143–7. [PubMed: 10102814]

[8]. Chilima TDP, Bovy T, Farid SS. Designing the optimal manufacturing strategy for an adherent allogeneic cell therapy. BioProcess International 2016;14(9):24–32.

[9]. Heathman TR, et al. Characterization of human mesenchymal stem cells from multiple donors and the implications for large-scale bioprocess development. Biochemical Engineering Journal 2016;108:14–23.

[10]. Lechanteur C, et al. Large-scale clinical expansion of mesenchymal stem cells in the GMP-compliant, closed automated Quantum(R) cell expansion system: comparison with expansion in traditional T-flasks. Stem Cell Research & Therapy 2014;4(8):1–11.

[11]. Wuchter P, et al. Standardization of Good Manufacturing Practice-compliant production of bone marrow-derived human mesenchymal stromal cells for immunotherapeutic applications. Cytotherapy 2015;17(2):128–39. [PubMed: 24856898]

[12]. Chinnadurai R, et al. Immune dysfunctionality of replicative senescent mesenchymal stromal cells is corrected by IFNgamma priming. Blood Adv 2017;1(11):628–43. [PubMed: 28713871]

[13]. Mendicino M, et al. MSC-based product characterization for clinical trials: an FDA perspective. Cell Stem Cell 2014;14(2):141–5. [PubMed: 24506881]

[14]. Lockhart RA, Aronowitz JA, Dos-Anjos Vilaboa S. Use of Freshly Isolated Human Adipose Stromal Cells for Clinical Applications. Aesthet Surg J 2017;37(suppl_3):S4–8.

[15]. Dykstra JA, et al. Concise Review: Fat and Furious: Harnessing the Full Potential of Adipose-Derived Stromal Vascular Fraction. Stem Cells Transl Med 2017;6(4):1096–108. [PubMed: 28186685]

[16]. Donnenberg AD, et al. Clinical implementation of a procedure to prepare bone marrow cells from cadaveric vertebral bodies. Regen Med 2011;6(6):701–6. [PubMed: 22050522]

[17]. Ahrens N, et al. Mesenchymal stem cell content of human vertebral bone marrow. Transplantation 2004;78(6):925–9. [PubMed: 15385815]

[18]. Cox G, et al. High abundance of CD271(+) multipotential stromal cells (MSCs) in intramedullary cavities of long bones. Bone 2012;50(2):510–7. [PubMed: 21807134]

[19]. Rybka WB, et al. Hematopoietic progenitor cell content of vertebral body marrow used for combined solid organ and bone marrow transplantation. Transplantation 1995;59(6):871–4. [PubMed: 7701582]

[20]. Soderdahl G, et al. Cadaveric bone marrow and spleen cells for transplantation. Bone Marrow Transplant 1998;21(1):79–84. [PubMed: 9486499]

[21]. Blashki D, et al. Mesenchymal stem cells from cortical bone demonstrate increased clonal incidence, potency, and developmental capacity compared to their bone marrow-derived counterparts. J Tissue Eng 2016;7:2041731416661196. [PubMed: 27579159]

[22]. Siclari VA, et al. Mesenchymal progenitors residing close to the bone surface are functionally distinct from those in the central bone marrow. Bone 2013;53 (2):575–86. [PubMed: 23274348]

[23]. Yusop N, et al. Isolation and Characterisation of Mesenchymal Stem Cells from Rat Bone Marrow and the Endosteal Niche: A Comparative Study. Stem Cells Int 2018;2018:6869128. [PubMed: 29765418]

[24]. Jones E, et al. Large-scale extraction and characterization of CD271+ multipotential stromal cells from trabecular bone in health and osteoarthritis: implications for bone regeneration strategies based on uncultured or minimally cultured multipotential stromal cells. Arthritis Rheum 2010;62(7):1944–54. [PubMed: 20222109]

[25]. Gorantla VS, et al. Development and validation of a procedure to isolate viable bone marrow cells from the vertebrae of cadaveric organ donors for composite organ grafting. Cytotherapy 2012;14(1):104–13. [PubMed: 21905958]

[26]. Li M, et al. Therapeutic Delivery Specifications Identified Through Compartmental Analysis of a Mesenchymal Stromal Cell-Immune Reaction. Sci Rep 2018;8(1):6816. [PubMed: 29717209]

[27]. Quah BJ, Warren HS, Parish CR. Monitoring lymphocyte proliferation in vitro and in vivo with the intracellular fluorescent dye carboxyfluorescein diacetate succinimidyl ester. Nat Protoc 2007;2(9):2049–56. [PubMed: 17853860]

[28]. Dominici M, et al. Minimal criteria for defining multipotent mesenchymal stromal cells. The International Society for Cellular Therapy position statement. Cytotherapy 2006;8(4):315–7. [PubMed: 16923606]

[29]. Gronthos S, et al. Molecular and cellular characterisation of highly purified stromal stem cells derived from human bone marrow. J Cell Sci 2003;116(Pt 9):1827–35. [PubMed: 12665563]

[30]. Simmons PJ, Torok-Storb B. Identification of stromal cell precursors in human bone marrow by a novel monoclonal antibody, STRO-1. Blood 1991;78(1):55–62. [PubMed: 2070060]

[31]. Dennis JE, et al. The STRO-1+ marrow cell population is multipotential. Cells Tissues Organs 2002;170(2–3):73–82. [PubMed: 11731697]

[32]. Bensidhoum M, et al. Homing of *in vitro* expanded Stro-1- or Stro-1+ human mesenchymal stem cells into the NOD/SCID mouse and their role in supporting human CD34 cell engraftment. Blood 2004;103(9):3313–9. [PubMed: 14715641]

[33]. Galipeau J, et al. International Society for Cellular Therapy perspective on immune functional assays for mesenchymal stromal cells as potency release criterion for advanced phase clinical trials. Cytotherapy 2016;18(2):151–9. [PubMed: 26724220]

[34]. Squillaro T, Peluso G, Galderisi U. Clinical Trials With Mesenchymal Stem Cells: An Update. Cell Transplant 2016;25(5):829–48. [PubMed: 26423725]

[35]. Eom YW, et al. The role of growth factors in maintenance of stemness in bone marrow-derived mesenchymal stem cells. Biochem Biophys Res Commun 2014;445(1):16–22. [PubMed: 24491556]

[36]. Galipeau J, Sensebe L. Mesenchymal Stromal Cells: Clinical Challenges and Therapeutic Opportunities. Cell Stem Cell 2018;22(6):824–33. [PubMed: 29859173]

[37]. Jossen V, et al. Manufacturing human mesenchymal stem cells at clinical scale: process and regulatory challenges. Appl Microbiol Biotechnol 2018;102(9):3981–94. [PubMed: 29564526]

[38]. Banfi A, et al. Replicative aging and gene expression in long-term cultures of human bone marrow stromal cells. Tissue Eng 2002;8(6):901–10. [PubMed: 12542936]

[39]. Baxter MA, et al. Study of telomere length reveals rapid aging of human marrow stromal cells following *in vitro* expansion. Stem Cells 2004;22(5):675–82. [PubMed: 15342932]

[40]. Bork S, et al. DNA methylation pattern changes upon long-term culture and aging of human mesenchymal stromal cells. Aging Cell 2010;9(1):54–63. [PubMed: 19895632]

[41]. Bruder SP, Jaiswal N, Haynesworth SE. Growth kinetics, self-renewal, and the osteogenic potential of purified human mesenchymal stem cells during extensive subcultivation and following cryopreservation. J Cell Biochem 1997;64(2):278–94. [PubMed: 9027588]

[42]. Digirolamo CM, et al. Propagation and senescence of human marrow stromal cells in culture: a simple colony-forming assay identifies samples with the greatest potential to propagate and differentiate. Br J Haematol 1999;107(2):275–81. [PubMed: 10583212]

[43]. Muraglia A, Cancedda R, Quarto R. Clonal mesenchymal progenitors from human bone marrow differentiate *in vitro* according to a hierarchical model. J Cell Sci 2000;113(Pt 7):1161–6. [PubMed: 10704367]

[44]. Redaelli S, et al. From cytogenomic to epigenomic profiles: monitoring the biologic behavior of *in vitro* cultured human bone marrow mesenchymal stem cells. Stem Cell Res Ther 2012;3(6):47. [PubMed: 23168092]

[45]. Moravcikova E, et al. Proteomic Profiling of Native Unpassaged and Culture-Expanded Mesenchymal Stromal Cells (MSC). Cytometry A 2018;93(9):894–904. [PubMed: 30211967]

[46]. Bara JJ, et al. Concise review: Bone marrow-derived mesenchymal stem cells change phenotype following *in vitro* culture: implications for basic research and the clinic. Stem Cells 2014;32(7):1713–23. [PubMed: 24449458]

[47]. Choi YH, Kim JK. Dissecting Cellular Heterogeneity Using Single-Cell RNA Sequencing. Mol Cells 2019;42(3):189–99. [PubMed: 30764602]

[48]. Hwang B, Lee JH, Bang D. Single-cell RNA sequencing technologies and bioinformatics pipelines. Exp Mol Med 2018;50(8):96.

[49]. Wu LW, et al. Donor age negatively affects the immunoregulatory properties of both adipose and bone marrow derived mesenchymal stem cells. Transpl Immunol 2014;30(4):122–7. [PubMed: 24632513]

[50]. Barreto-Duran E, et al. Impact of donor characteristics on the quality of bone marrow as a source of mesenchymal stromal cells. Am J Stem Cells 2018;7(5):114–20. [PubMed: 30697455]

[51]. Beane OS, et al. Impact of aging on the regenerative properties of bone marrow-, muscle-, and adipose-derived mesenchymal stem/stromal cells. PLoS One 2014;9 (12):e115963. [PubMed: 25541697]

[52]. Katsara O, et al. Effects of donor age, gender, and *in vitro* cellular aging on the phenotypic, functional, and molecular characteristics of mouse bone marrow-derived mesenchymal stem cells. Stem Cells Dev 2011;20(9):1549–61. [PubMed: 21204633]

[53]. Baker N, Boyette LB, Tuan RS. Characterization of bone marrow-derived mesenchymal stem cells in aging. Bone 2015;70:37–47. [PubMed: 25445445]

[54]. Schimke MM, Marozin S, Lepperdinger G. Patient-Specific Age: The Other Side of the Coin in Advanced Mesenchymal Stem Cell Therapy. Front Physiol 2015;6:362. [PubMed: 26696897]

[55]. Charif N, et al. Aging of bone marrow mesenchymal stromal/stem cells: implications on autologous regenerative medicine. Biomed Mater Eng 2017;28(s1):S57–63. [PubMed: 28372278]

[56]. Arshad A, Anderson B, Sharif A. Comparison of organ donation and transplantation rates between opt-out and opt-in systems. Kidney Int 2019;95 (6):1453–60. [PubMed: 31010718]

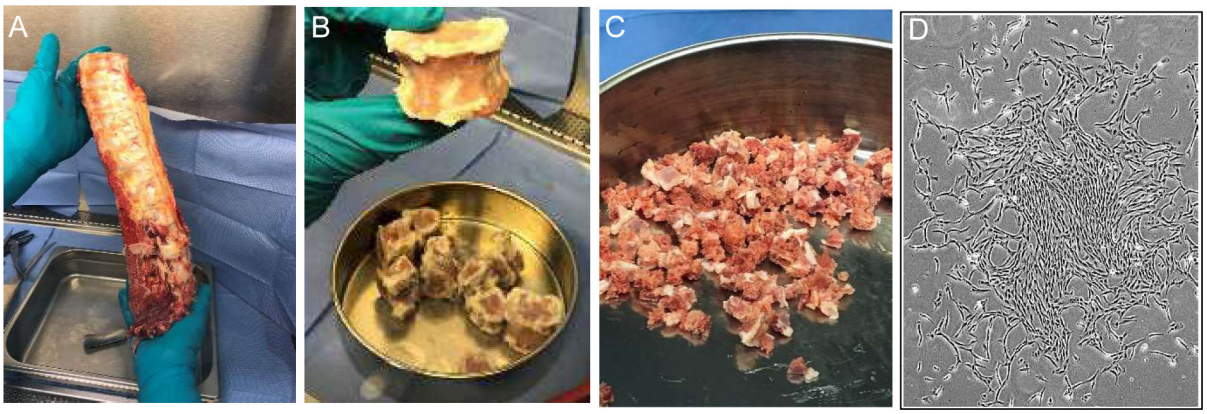


**Figure 1.**

Processing of a typical vertebral column to isolate vBA-MSCs. Vertebrae (typically T8 L5) were cleaned of soft tissue (A) before separating VBs and removing disks and remaining soft tissues (B). VBs were ground to approximately 1.5 $cm^3$ fragments (C) before enzymatic digestion to release adherent cells. (D) Plastic-adherent vBA-MSCs form typical spindle shapes (passage 2 cells) in culture.

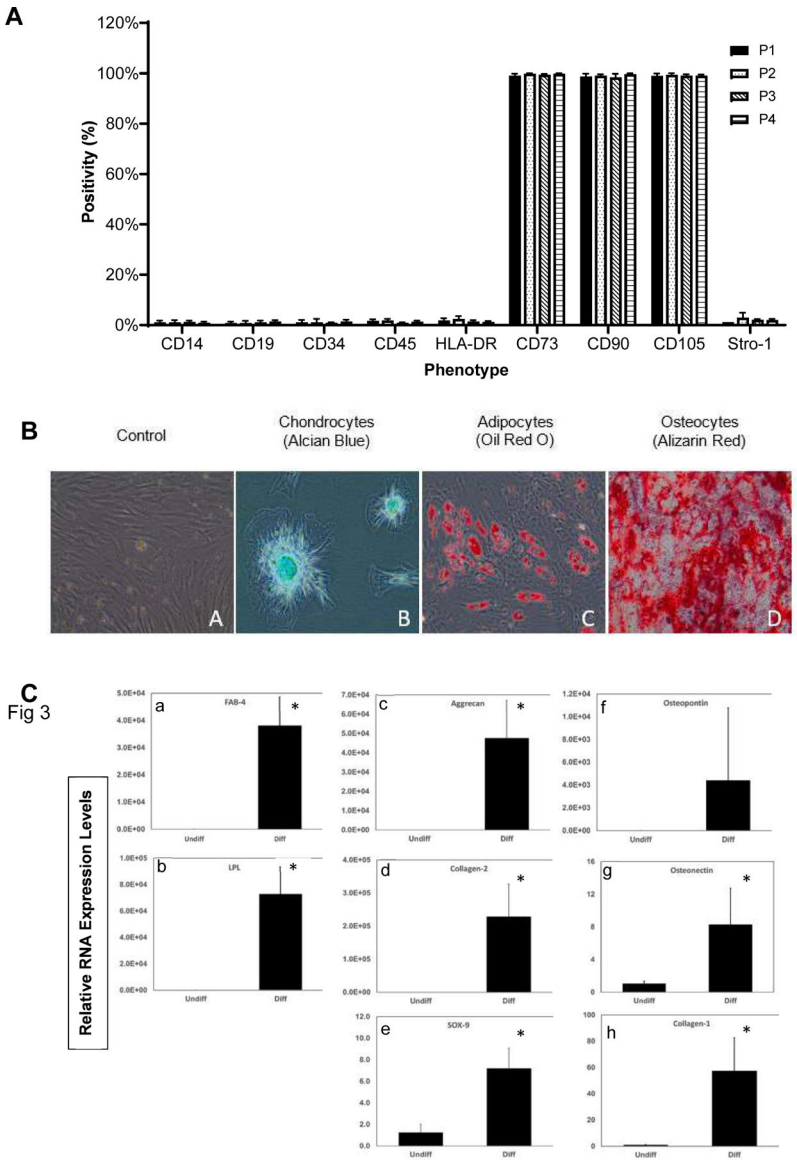


**Figure 2.**

Surface antigen phenotype and trilineage differentiation of vBA-MSCs. (A) Passage 1, 2, 3 and 4 vBA-MSCs from 3 different donors (DD1, DD2 and DD3; donor characteristics listed in Table 1) were analyzed for surface antigen expression using fluorescently conjugated antibodies and flow cytometry. The percentage of cells (gated on whole cells using side and forward scatter) after culturing for each passage is shown. (B) Passage 3 vBA-MSCs grown in expansion medium (far left); or (from left to right) induced to undergo either chondrogenesis, adipogenesis or osteogenesis. Images were captured after staining for chrondocytes (Alcian Blue), adipocytes (Oil Red O) or osteocytes (Alizarin Red), as described in Methods. Images are representative of results with the 3 different donor-derived vBA-MSCs. Magnification for all 20X. (C) Quantitation of differentiation by analysis of adipogenic (LPL and FABP4), chondrogenic (aggrecan, collagen 1 and SOX9) and osteogenic (osteopontin, osteonectin and collagen 1) RNA markers in Undiff

and Diff vBA-MSC cultures by quantitative RT-PCR. Relative mRNA levels are shown. Unpaired Student's *t*-test comparing undifferentiated with differentiated cells. $*P < 0.05$. DD, deceased donor; Diff, differentiated; FABP4, fatty acid binding protein 4; LPL, lipoprotein lipase; mRNA, messenger RNA; RT-PCR, real-time polymerase chain reaction; Undiff, undifferentiated.

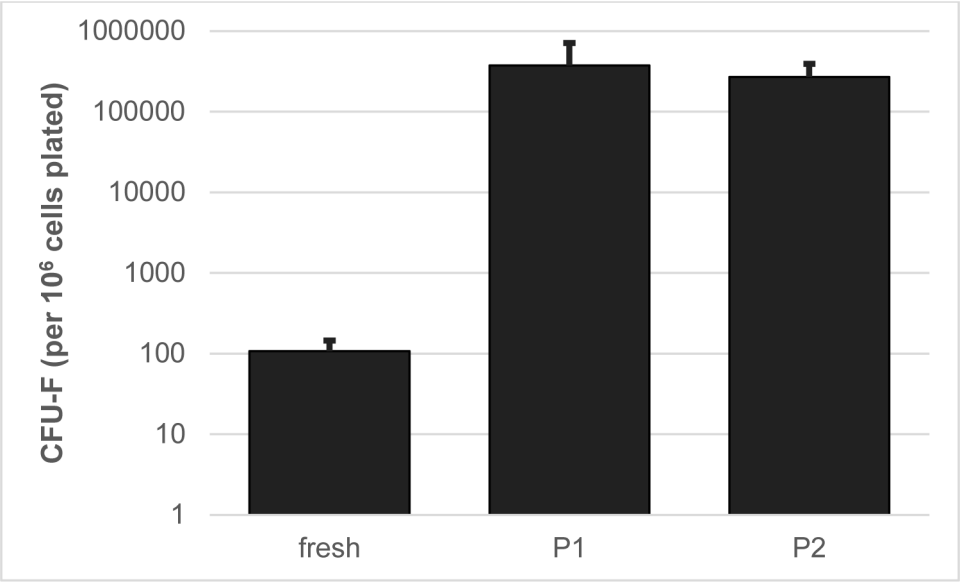


**Figure 3.**

CFU-F potential of vBA-MSCs isolated from 3 different donors (DD1, DD2 and DD3; donor characteristics listed in Table 1) and plated immediately after isolation by digestion (fresh) or after 1 or 2 passages (P1 and P2). Both $5 \pm 10^5$ (fresh) and 624 (passaged) total cells from each of 3 donors were plated in triplicate wells of a 6-well plate and incubated for 14 days, with media changes every 3–4 days.

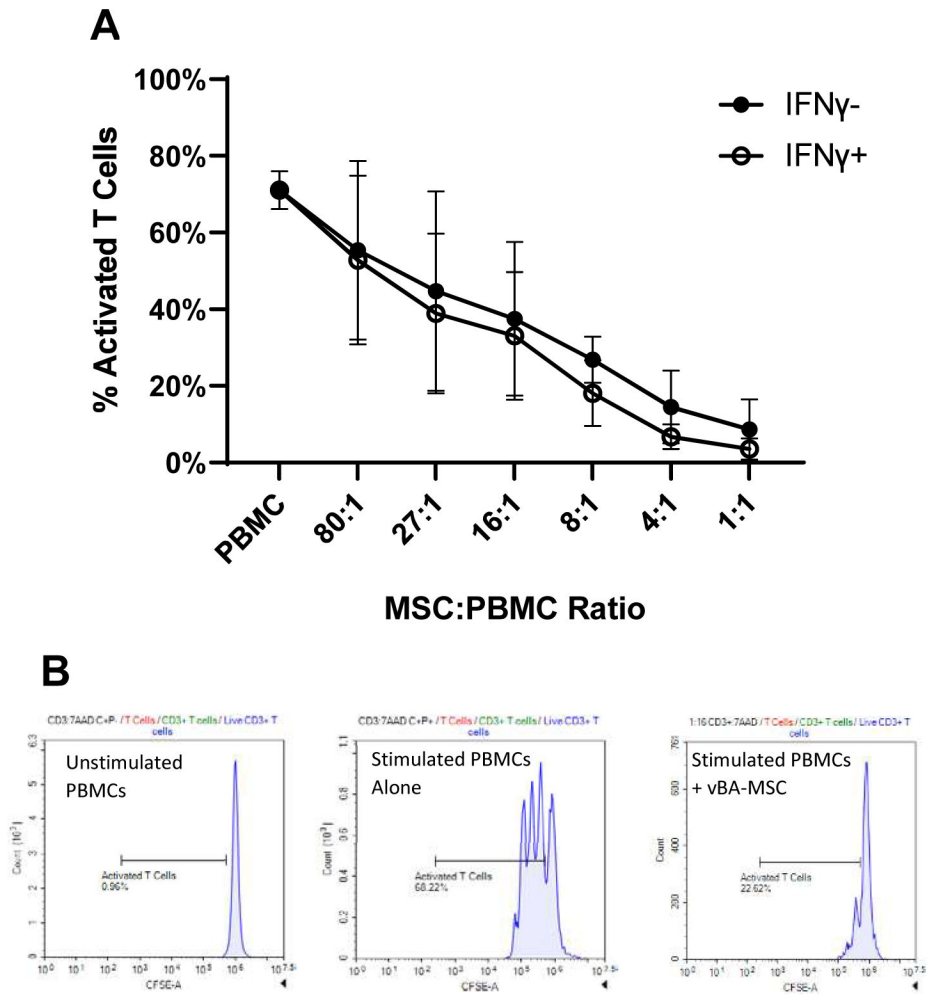


**Figure 4.**

VBA-MSC suppression of T-cell activation. (A) Suppression at decreasing ratios of PBMCs to vBA-MSCs. PBMCs isolated from the blood of a single donor were labeled with CSFE. The vBA-MSCs were allowed to adhere 2 h in 96-well plates before washing and adding 4 × 105 PBMCs. In some experiments IFN-$\gamma$ (100 ng/mL) was added 18–24 h before adding PBMCs. T cells were stimulated for 4 days with PHA. Cells were recovered from the plates and analyzed by flow cytometry after labeling with anti-CD3-PE antibodies. The percentage of activated T cells is plotted. (B) Representative flow plots for PBMCs alone without and with PHA activation as well as PBMCs and MSCs after PHA activation are shown. Each data point represents the mean of 3 different experiments with 3 different donors (DD1, DD2 and DD3). Error bars represent the standard deviation. $P > 0.05$ for comparisons of all ratios of PBMCs to vBA-MSCs +/- IFN-$\gamma$. CSFE, carboxyfluorescein diacetate succinimidyl ester; DD, deceased donor.

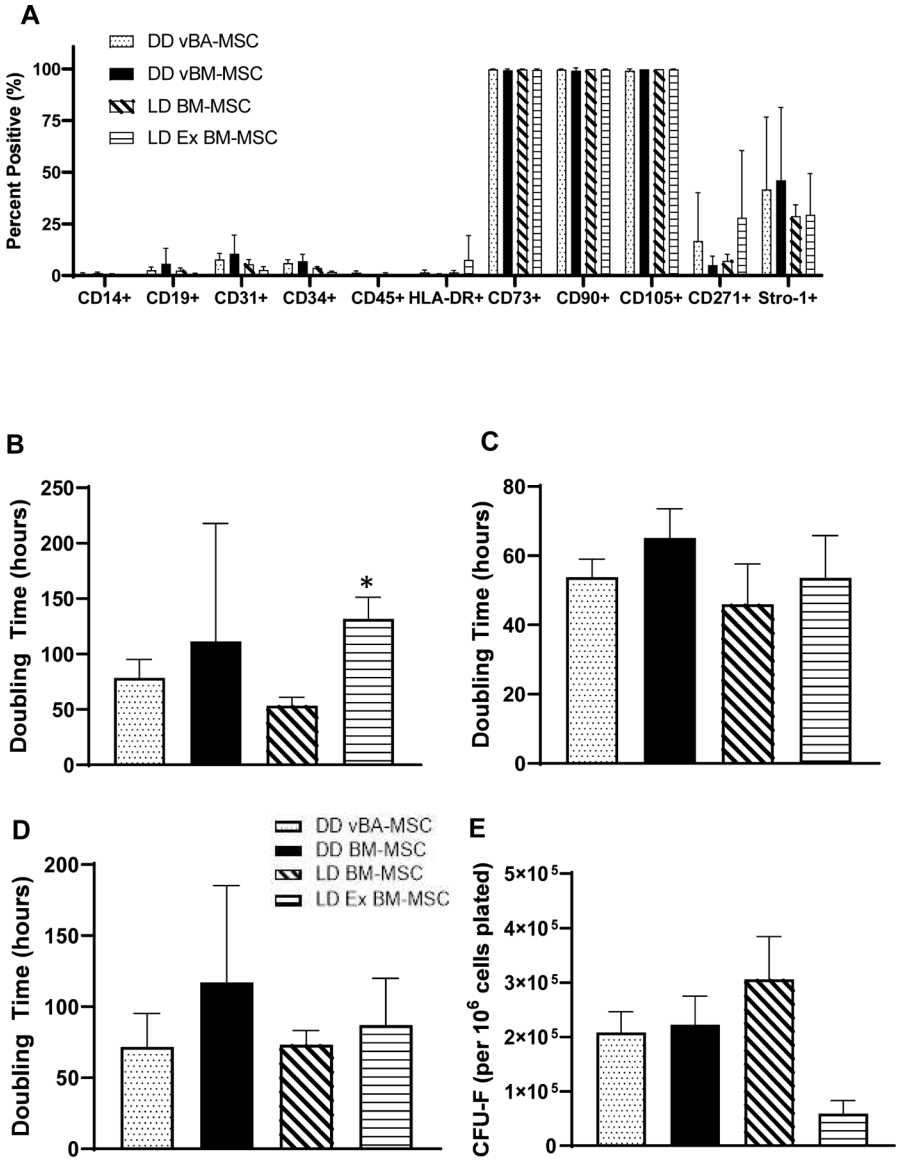


**Figure 5.**

Comparison of vBA-MSCs with BM-MSCs. (A) Surface marker expression of passage 3 cells was characterized by flow cytometry. The different sources of MSCs were DD vBA-MSCs, DD BM-MSCs, LD BM-MSCs and LD Ex BM-MSCs obtained from a commercial source at passage 2. The percentage of cells within the total population after gating out debris is shown. There were no differences in surface marker expression between cell types. (B–D) Comparison of PDTs from passages 2 to 3 (B), 3 to 4 (C) and 4 to 5 (D). Ex LD BM-MSCs grew significantly slower between passages 2 and 3 than either vBA-MSCs or LD BM-MSCs. No difference in PDT was observed in the subsequent 2 passages. (E) CFU-F assays were performed as described in Figure 3 for passaged cells. Formation of CFU-F was significantly lower for passage 2 Ex LD BM-MSCs compared with the other 3 sources of MSCs (also at passage 2). Each bar represents the mean ± SD of the 3 donors for each MSC source. The specific donors were LD BM-MSCs (donors LD1, LD2 and LD3),

LD Ex BM-MSCs (donors LD4, LD5 and LD6), vBM-MSCs and vBA-MSCs (donors DD1, DD2 and DD3). Donor characteristics are listed in Table 1. *$P < 0.05$. DD, deceased donor; SD, standard deviation.

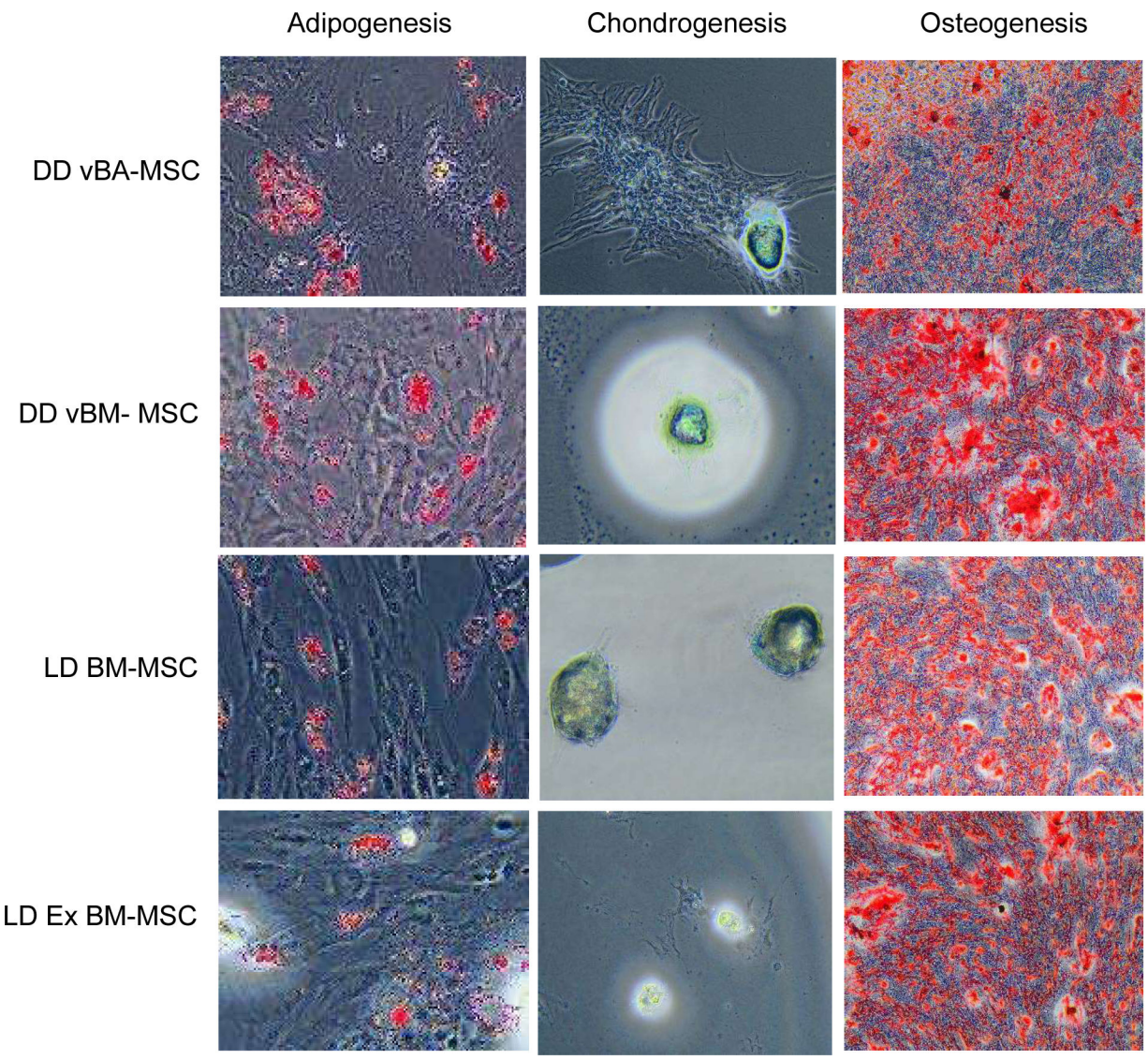


**Figure 6.**

Trilineage differentiation of vBA-MSCs and MSCs isolated from DD VB BM and BM aspirated from the iliac crests of living donors. Cells were cultured and induced to undergo differentiation for each cell type as described in Figure 2. There were no qualitative differences in adipogenic, chondrogenic or osteogenic potential of passage 3 cells from any of the 4 sources. Images are representative of experiments with the 3 different donors for each source of MSCs. Magnification is indicated on each image. DD, deceased donor.

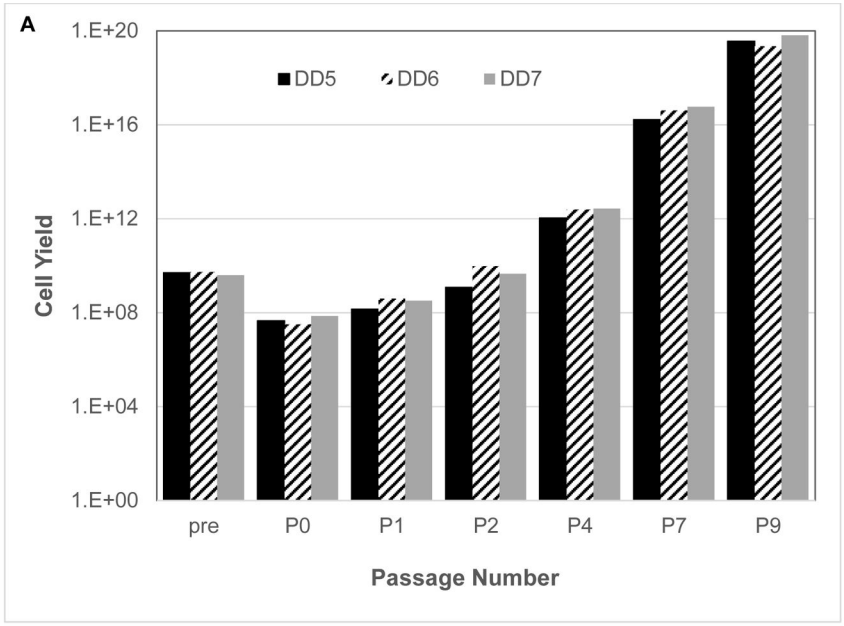


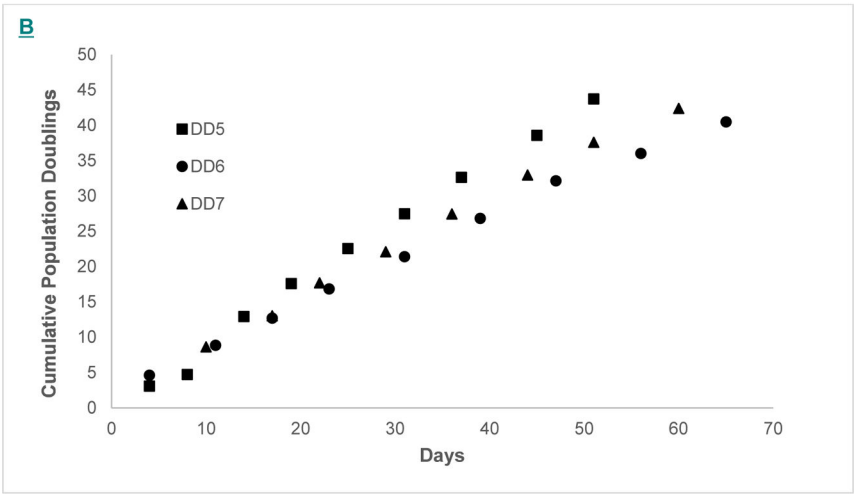


**Figure 7.**

Cumulative population growth of vBA-MSCs from 3 different donors. The vBA-MSCs obtained from digested fragments (5 g) of VBs from 3 donors (DD5, DD6 and DD7) were isolated and expanded to passage 1 to form an MCB. A portion of the passage 1 vBA-MSCs from each donor was expanded to passage 9. (A) Observed and potential cumulative growth yields at each passage of vBA-MSCs from 3 donors. (B) Cumulative vBA-MSC population doublings at passages 0–9. PDs were calculated based on initial numbers of cells plated and the number recovered after each plate reached 80% confluency before replating the cells and were used to determine the theoretical total cell yield after each passage. Theoretical total yields at passages 2–9 were obtained by exponentiating (base 2) the PD calculated for each passage and multiplying by the cumulative cell number from each preceding passage. Each donor vBA-MSC was plated in triplicate for each passage. The CV between cell numbers

obtained from each well was <15%. CV, coefficient of variation; DD, deceased donor; PD, population doubling.

**Table 1.**

Description of donors used in this study

| Donor ID | Recovered MSC | Age | Sex | Race/ Ethnicity |
|---|---|---|---|---|
| DD1[1] | vBA-MSC, vBM-MSC | 22 | M | Caucasian |
| DD2 | vBA-MSC, vBM-MSC | 13 | M | Caucasian |
| DD3 | vBA-MSC | 35 | M | Hispanic |
| DD4 | vBA-MSC, vBM-MSC | 19 | M | Hispanic |
| DD5 | vBA-MSC | 17 | M | Caucasian |
| DD6 | vBA-MSC | 14 | M | Caucasian |
| DD7 | vBA-MSC | 23 | M | Caucasian |
| LD1 | LD BM-MSC | 20 | F | African American |
| LD2 | LD BM-MSC | 23 | F | African American |
| LD3 | LD BM-MSC | 28 | M | African American |
| LD4 | Ex LD BM-MSC | 24 | F | African American |
| LD5 | Ex LD BM-MSC | 36 | M | African American |
| LD6 | Ex LD BM-MSC | 25 | M | African American |

[1]Abbreviations: DD, deceased donor; LD, live donor; vBM-MSC, vertebral bone marrow-MSC; vBA-MSC, vertebral bone-adherent MSC,